EurJOC European Journal of Organic Chemistry

FULL PAPER

DOI: 10.1002/ejoc.201201633

Foldameric β-H18/20$_P$ Mixed Helix Stabilized by Head-to-Tail Contacts: A Way to Higher-Order Structures

Éva Szolnoki,[a] Anasztázia Hetényi,[b] István M. Mándity,[a] Ferenc Fülöp,[a] and Tamás A. Martinek*[a]

Keywords: Helical structures / Protein folding / Self-assembly / Foldamers / Amino acids / Peptides

Peptidic foldamers are known to exhibit increased diversity in the periodic secondary-structure space in comparison with their natural counterparts, but their higher-order self-organization has been studied less thoroughly. In theory, large-diameter peptide foldamer helices have the capability of self-recognition through axial helix–helix interactions (e.g., head-to-tail), but this phenomenon has previously been observed in only one instance. In this article we report on the discovery of the largest-diameter β-peptidic mixed helix to date, the H18/20$_P$ helix. Its formation is solvent-dependent and its folding occurs cooperatively through head-to-tail self-assembly in solution. These findings suggest that axial helix–helix interactions can serve as a new mode for the formation of tertiary/quaternary structures for peptide foldamers, which also show higher-order structural diversity than natural proteins.

Introduction

Foldamers, a class of self-organizing polymers, continue to attract interest as biomimetic[1–4] and bioactive materials.[2,5–19] Although the formation of secondary structures of peptidic foldamers has been thoroughly studied, their higher-order self-organization (tertiary and quaternary structures) and its effects on the folding propensities are less well understood. It has been shown that peptidic foldamers are able to fold cooperatively into helix bundles;[20] β- and α,β-peptide sequences that were disordered at low concentrations have recently been shown to form quaternary structures through self-assembling helical building blocks.[21–24] Infinite pleated sheet aggregates were also observed, which eventually appeared in the form of nanostructured fibrils.[25–29] These processes are very similar to those leading to the formation of solvophobic interaction-driven tertiary/quaternary structures observed for natural proteins. Although peptidic foldamers exhibit greatly increased diversity in the periodic secondary-structure space as compared with their natural counterparts, the question of whether these intriguing sequences are able to demonstrate modes of cooperative folding that have previously not been seen or only rarely for natural chains is still under investigation.

Peptidic foldamers have the ability to form helices with relatively large diameters,[30,31] which, in theory, can participate in stable axial (e.g., head-to-tail) interactions through backbone hydrogen bonds and side-chain interactions. This phenomenon can be observed in gramicidin A, for example, in which axial self-recognition takes place in the membrane environment.[32] In peptidic foldamers, axial helix–helix interactions were recently observed in the self-association of the β-peptidic H12 helix to form the large-diameter β-H18 helix.[33] In this work we report on the serendipitous discovery of the largest-diameter β-peptidic mixed helix known to date, the β-H18/20 helix, the formation of which is solvent-dependent and its folding occurs cooperatively through head-to-tail interactions in solution.

Results and Discussion

The β-H10/12 helix,[34] constructed from *cis*-2-aminocyclopentanecarboxylic acid (*cis*-ACPC) units,[28] is a pseudo-symmetric system. Its stereochemically alternating backbone can geometrically form both right- and left-handed helices, but the sequence [(1*S*,2*R*)-ACPC-(1*R*,2*S*)-ACPC]$_3$-NH$_2$ (**1**) forms only the stable β-H10/12$_P$ helix (right-handed). For stereochemical reasons, inversion of the backbone configurations of the sequence results in the mirror image (**2**), which should form an *M*-type helix (left-handed). According to the stereochemical patterning approach introduced earlier,[30,31] this operation is equivalent to shifting of the backbone configuration pattern with a monomer unit. Our starting hypothesis was that manipulation of either the C or N terminus would result in a deterministic transfer of chiral information along the chain by changing the helix sense, but that the H10/12 helical structure would be retained. It has been repeatedly shown that the N terminus

[a] Institute of Pharmaceutical Chemistry, University of Szeged, Eötvös u. 6, 6720 Szeged, Hungary
Fax: +36-62-545705
E-mail: martinek@pharm.u-szeged.hu
Homepage: http://www2.pharm.u-szeged.hu/martinek-group/
[b] Department of Medical Chemistry, University of Szeged, Dóm t. 13, 6720 Szeged, Hungary
Supporting information for this article is available on the WWW under http://dx.doi.org/10.1002/ejoc.201201633.

of a peptidic chain has a profound effect on its propensity towards helix formation[35,36] and the helical sense.[37,38] To test the presumed effects of changing the N terminus on the handedness of the β-H10/12 helix, new sequences were synthesized (Scheme 1) by the *N*-capping of **2** with an acetyl group (**3**), a stereochemically matching *cis*-ACPC (**4**) or by the *N*-capping of **4** with an acetyl group (**5**). These compounds were synthesized on a solid support by means of Fmoc chemistry.

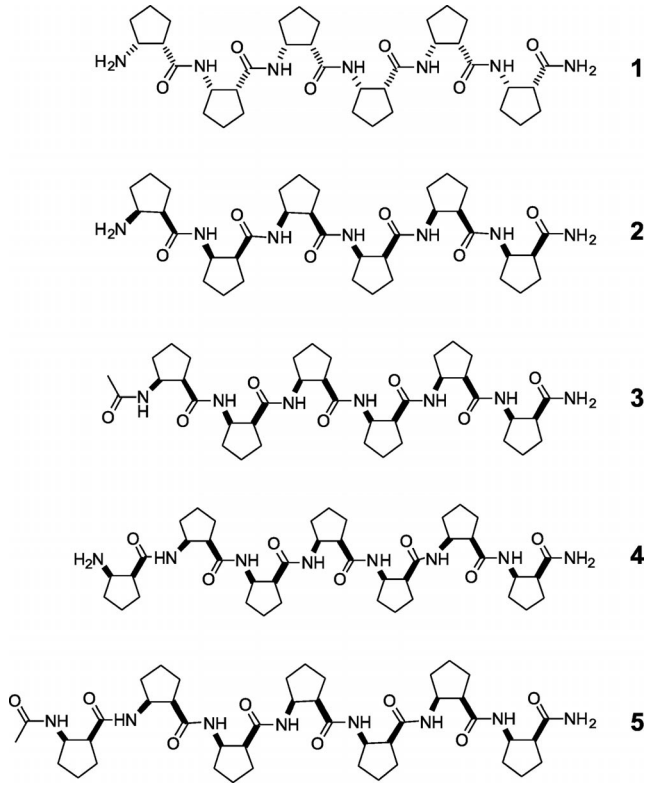

Scheme 1. Structures of **1**–**5** studied for their helicity.

The effects of *N*-capping were monitored first by electronic circular dichroism (ECD) spectroscopy. It is clear from the data obtained for **1** and **2** that the frame-shift in the configuration pattern results in mirror-image ECD spectra (Figure 1), which indicates the expected opposite handedness (left) of the β-H10/12$_M$ helix. Acetylation of the N terminus furnished a similar, but considerably lower-intensity Cotton effect for **3**, which may indicate that the β-H10/12 conformation is still present, but either the amount of disorder has increased or both the right- and left-handed conformations are present. For **4**, the additional stereochemically matching *cis*-ACPC unit at the N terminus led to a positive Cotton effect, which indicates that it is a right-handed helix. *N*-Acetylation of the this chain (**5**) again led to the predominance of a left-handed helix, but the ECD response was of lower intensity. These findings support our hypothesis that the N terminus plays a crucial role in the formation of the β-H10/12 helix and that control over the handedness of the helix can be achieved by manipulating the N-terminal residue.

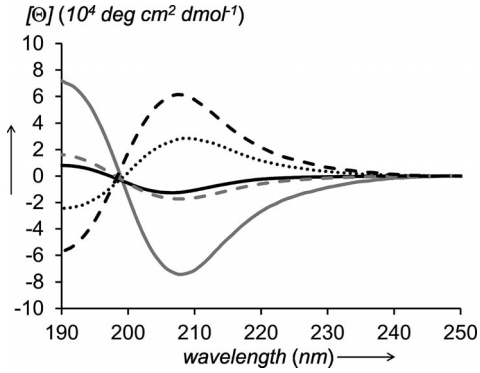

Figure 1. ECD spectra recorded in MeOH for a 1 mM solution of **1** (dashed black, taken from ref.[28]), **2** (solid gray), **3** (solid black), **4** (dotted black) and **5** (dashed gray).

NMR investigations revealed good signal resolution for **2**–**5**, and direct measurement of the NH/ND exchange rates in CD_3OD indicated the presence of predominantly folded structures (see Figures S1–S4 in the Supporting Information). Relatively high exchange rates were observed for **3**, but the signal decay was still acceptable for an overall folded state. This was supported by the ECD and NOE results. ROESY experiments were performed to acquire high-resolution structural data. Characteristic $C_\beta H_i$–NH_{i+2} (i = even number) and NH_i–$C_\beta H_{i+2}$ (i = odd number) long-range NOE interactions were observed for **2**, **3** and **5** in both CD_3OH and [D_6]DMSO, which strongly supports the predominance of the H10/12$_M$ (left-handed) helix. In addition, the vicinal couplings for NH_i–$C_\beta H_i$ are in good agreement with the H10/12$_M$ helix (see Tables S1 and S2 in the Supporting Information). Cross-peaks relating to the *P* helix (right-handed) or other inconsistent NOE interactions were not observed. This indicates that the relatively low ECD intensities exhibited by the acetylated chains are not a result of significant disorder or multiple conformations.

Analysis of the ROESY spectra revealed solvent-dependent NOE patterns for **4**. Previously unreported NOE interactions were observed in CD_3OH: long-range NOEs arising from $C_\beta H_i$–NH_{i+4} (i = odd) and NH_i–$C_\beta H_{i+4}$ (i = even) interactions could be clearly identified (Figure 2 and Figure S5 in the Supporting Information). Furthermore, $C_\alpha H_1$–$C_\beta H_6$, $C_\beta H_3$–NH_7 and NH_4–$C_\beta H_6$ NOE contacts could be observed (Figure 2). The initial structure refinement with a single chain and the full set of NOE-derived distance restraints revealed that the regular i–i+4 interactions are mutually exclusive with the last three NOEs. Because the $^3J(NH_i–C_\beta H_i)$ couplings exhibit the pattern expected for a well-folded mixed helix (see Table S3 in the Supporting Information) and the NH/ND exchange rates are low (Figure S3), we adopted the hypothesis that the outlier NOEs are of interchain origin. The repeated conformational search with only the regular i–i+4 restraints and subsequent manual docking of the secondary structure units led to the conclusion that the observed NOE pattern is in full agreement with H18/20$_P$ (right-handed) helices assembled through head-to-tail interactions (Figure 3). This

finding is in accord with the positive Cotton effect observed in the ECD spectrum, the intensity of which cannot be directly compared with those of **1** and **2**. In contrast to the observations in CD_3OH, only *i*–*i*+2 NOEs were observed for **4** in [D_6]DMSO. Some of the interactions (NH_1–$C_\beta H_3$, $C_\beta H_2$–NH_{i+4} and $C_\beta H_4$–NH_{i+6}) indicate the presence of an H10/12$_P$ helix, but a $C_\beta H_5$–NH_{i+7} interaction was found at the C terminus, which is a sign of an *M*-type fold. The undetermined secondary structure could also be seen in the loss of the alternating pattern of the $^3J(NH_i$–$C_\beta H_i)$ values. The most likely explanation for this lies in the presence of both screw senses and partially folded states along the chain because N-terminal helix nucleation is less effectively propagated in [D_6]DMSO. Moreover, the NMR findings support the view that the formation of the large-diameter H18/20$_P$ helix is coupled to the head-to-tail association in CD_3OH. The high-resolution model in Figure 3 reveals that the helix–helix interactions are stabilized by four interchain hydrogen bonds, NH_8–NH_1, NH_2–CO_5, NH_7–CO_2 and NH_4–CO_7, which are efficiently disrupted in the chaotropic [D_6]DMSO.

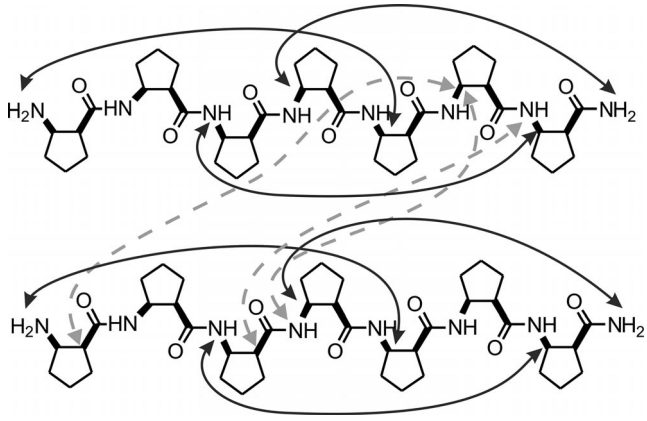

Figure 2. NOE interactions observed in CD_3OH for **4**. Black arrows indicate intramolecular *i*–*i*+4 contacts, which supports right-handed β-H18/20$_P$ helical geometry, and gray dashed arrows indicate head-to-tail helix–helix NOEs arising from self-association.

The helical self-association of **4** in CD_3OH was further investigated by concentration-dependent DOSY NMR spectroscopy. The apparent aggregation number was 3 at a concentration of 100 μM, which rose to 8 at 1 mM (see Figure S6 in the Supporting Information). Sequences **2**, **3** and **5** did not exhibit self-association in the solution phase.

To explore the effect of self-association on the secondary structure, concentration-dependent ECD spectra were recorded (Figure 4). Upon dilution in the range 1 mM to 100 μM, no significant change was observed. Although the DOSY NMR spectroscopic data indicate a decreasing aggregation number, the interchain association was still predominant, as reflected in the ECD spectra. Below 100 μM, the concentration had a marked effect on the ECD response, the normalized intensity of the positive band decreased and a redshift of the Cotton effect was detected. Unfortunately, high-resolution structure could not be determined at 10 μM. We speculate that the observed ECD spectrum can be explained by increasing disorder as the structure partially refolds into the H10/12 helix, possibly forming both *P* and *M* helices, a phenomenon similar to that found in [D_6]DMSO. These findings strongly support the view that head-to-tail self-association makes a crucial contribution to the stability of the large-diameter H18/20$_P$ helix and that axial helix–helix interactions occur in a cooperative manner.

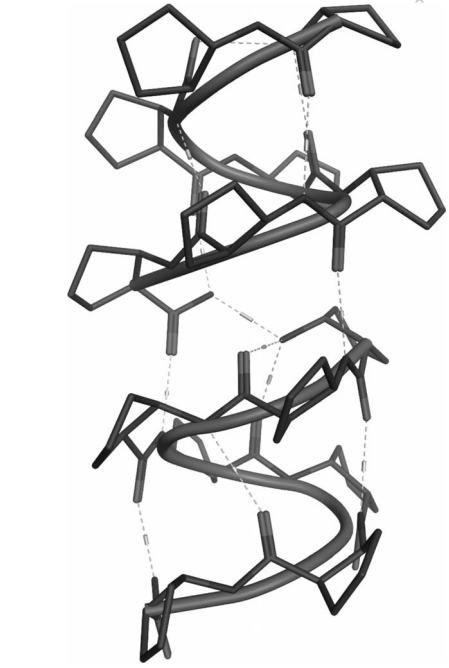

Figure 3. β-H18/20$_M$ mixed helix head-to-tail dimer of **4** obtained by NMR structure refinement in CD_3OH and a final ab initio geometry optimization at the B3LYP/6-311G** level of theory.

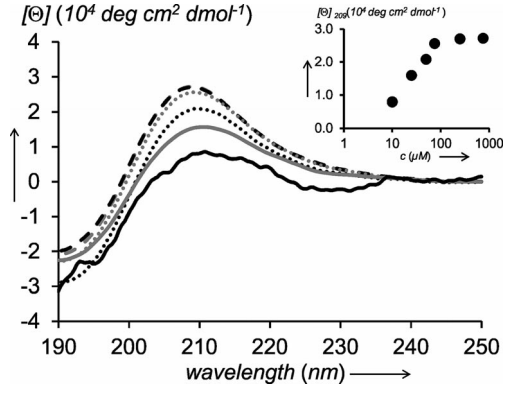

Figure 4. Concentration-dependent ECD spectra of **4** in MeOH. Data were recorded at concentrations of 10 (solid black), 25 (solid gray), 50 (dotted black), 75 (dotted gray), 250 (dashed black) and 750 μM (dashed gray). Inset: mean residue ellipticities measured at 209 nm.

Conclusions

In accordance with our starting hypothesis, manipulation of the N terminus of **2** resulted in a deterministic transfer

of chiral information along the mixed helix by changing the helicity of the chain. This phenomenon, however, could also be observed by changing the chain length and solvent. *N*-Acetylation of the left-handed hexameric sequence (**3**) changed neither the helix geometry nor the screw sense. Elongation of the chain at the N terminus with a stereochemically matching *cis*-ACPC residue (**4**) resulted in a predominantly right-handed helix conformation in MeOH. Moreover, concentration-dependent refolding to yield β-H18/20$_P$ was observed, which is the largest-diameter foldameric helix described so far. Although the β-H10/12 helix and its screw sense were affected by the terminal residue in DMSO, stereochemical information did not fully propagate along the chain in this chaotropic solvent. The NMR results obtained in CD_3OH strongly suggest a head-to-tail helix–helix association, and the concentration-dependent ECD spectra provided evidence for the cooperative formation of a secondary structure and self-assembly. Together with our earlier observations on the head-to-tail interactions and self-association accompanying the formation of the β-H18 helix, we can conclude that these coupled folding and self-assembly processes with axial helix–helix interactions offer a general route to the formation of tertiary/quaternary structures for these large-diameter foldameric helices.

Experimental Section

Peptide Synthesis: Foldamers **2**–**5** were synthetized by using a standard solid-phase technique involving 9*H*-fluoren-9-ylmethoxycarbonyl (Fmoc) chemistry. The peptide chains were elongated on TentaGel R RAM resin (0.19 mmol g^{-1}) and the syntheses were carried out manually on a 0.1 mmol scale. Couplings were performed with HATU/DIPEA {HATU = [2-(7-aza-1*H*-benzotriazol-1-yl]-1,1,3,3-tetramethyluronium hexafluorophosphate, DIPEA = *N*,*N*-diisopropylethylamine} without difficulties. The peptide sequences were cleaved from the resin with 95% trifluoroacetic acid (TFA) and 5% H_2O at room temperature for 3 h. The TFA was then removed and the resulting free peptides were solubilized in aqueous AcOH (10%), filtered and lyophilized. The crude peptides were investigated by RP-HPLC, using a Phenomenex C18 column (4.6 × 250 mm). The solvent system used was TFA (0.1%) in water (A), TFA (0.1%) and MeCN (80%) in water (B); gradient: 5→100% B over 35 min, flow rate 1.2 mL min^{-1}, detection at 206 nm. The above peptides were purified on an HPLC system with a Phenomenex C18 column (10 × 250 mm). The appropriate fractions were pooled and lyophilized. The purified peptides were characterized by mass spectrometry with an Agilent 1100 LC-MSD trap mass spectrometer equipped with an electrospray ion source. The spectra were recorded in positive ionization mode, scanning in the range *m*/*z* = 100–2200. The following molecular weights were determined: **2**: *m*/*z* = 684.6 $[M + H]^+$; **3**: *m*/*z* = 726.6 $[M + H]^+$; **4**: *m*/*z* = 795.7 $[M + H]^+$; **5**: *m*/*z* = 837.7 $[M + H]^+$.

NMR Experiments: NMR measurements were performed with a Bruker Avance III 600 MHz spectrometer with a multinuclear probe with a z-gradient coil in 0.1–1 mM CD_3OH and [D_6]DMSO solutions at 298 K. The ROESY measurements were carried out with the WATERGATE solvent suppression scheme for the ROESY spinlock and mixing times of 225 and 400 ms were used; the number of scans was 64. The TOCSY measurements were performed with homonuclear Hartmann–Hahn transfer with the MLEV17 sequence with a mixing time of 80 ms; the number of scans was 32. For all the 2D NMR spectra, 2024 time domain points and 512 increments were applied. Processing was carried out by using a cosine-bell window function with single zero-filling and automatic baseline correction. The DOSY (PFGSE) NMR measurements were performed by using the stimulated echo and longitudinal eddy current delay (LED) sequence with water suppression. A time of 2 ms was used for the dephasing/refocusing gradient pulse length (δ) and 250 ms for the diffusion delay (Δ). The gradient strength was changed quadratically (from 5 to 60–95% of the maximum value with a B-AFPA 10 A gradient amplifier) and the number of steps was 16. Each measurement was performed with 64 scans and 2K time domain points. For the processing, an exponential window function and single zero-filling were applied. During the diffusion measurements, the temperature fluctuation was less than 0.1 K. Prior to the NMR scans, all the samples were equilibrated for 30 min. DOSY spectra were processed and evaluated by using the exponential fit implemented in Topspin 3.1.[39] The aggregation numbers were calculated from the Stokes–Einstein equation and cholesterol was utilized as an external volume standard.

ECD Spectroscopy: ECD spectra were measured with a Jasco J815 spectrometer at 25 °C in a 0.02 cm cell. The baseline spectrum recorded of only the solvent was subtracted from the raw data. The concentration of the sample solutions was 1 mM and for the concentration-dependent measurements, concentrations of 25 μM to 1 mM were used in CD_3OH. Ten spectra were accumulated for each sample. Molar ellipticity, [Θ], is given in units of deg cm^2 dmol^{-1}. The data were normalized for the oligomer concentration and the number of chromophores.

Molecular Mechanics Calculations: Molecular mechanics simulations were carried out in the Molecular Operating Environment (MOE) of the Chemical Computing Group. For the energy calculations, the MMFF94x force-field was used without a cut-off for van der Waals or coulombic interactions, and the distance-dependent dielectric constant (ε_r) was set to ε = 1.8 (corresponding to MeOH). Conformational sampling was performed by hybrid Monte–Carlo (MC) molecular-dynamics (MD) simulation (as implemented in MOE) at 300 K with a random MC sampling step after every 10 MD steps. The MC–MD simulation was run with a step size of 2 fs for 20 ns, and the conformations were saved after every 1000 MD steps, which resulted in 10^4 structures. For the NMR-restrained simulation, the upper distance limits were calculated by using the isolated spin-pair approximation and classified according to the standard method (strong 2.5 Å, medium 3.5 Å and weak 5 Å). The lower limit was set to 1.8 Å. Restraints were applied as a flat-bottomed quadratic penalty term with a force constant of 5 kcal Å^{-2}. The final conformations were minimized to a gradient of 0.05 kcal mol^{-1} and the minimization was applied in a cascade manner by using the steepest-descent conjugate gradient and truncated Newton algorithm.

Ab Initio Calculations: The optimizations were carried out in two steps by using the Gaussian 09[40] program: first by using the HF/3-21G basis set and then by using density-functional theory at the B3LYP/6-311G** level of theory with a default set-up.

Supporting Information (see footnote on the first page of this article): NH/ND exchange, TOCSY and ROESY spectra, DOSY NMR data and scalar couplings for all sequences studied, ECD spectra recorded in H_2O, ab initio geometries, HPLC, ESI-MS, ^{1}H and ^{13}C NMR characterizations together with NMR assignments.

Acknowledgments

This work was supported by the European Union (EU) (COST Action CM0803), the Hungarian Research Foundation (OTKA PD83600 and K83882), and the Hungarian Academy of Sciences (Lendulet programme, LP-2011-009). E. S. acknowleges support by the Gedeon Richter Centennial Foundation.

[1] G. Guichard, I. Huc, *Chem. Commun.* **2011**, *47*, 5933.
[2] W. S. Horne, S. H. Gellman, *Acc. Chem. Res.* **2008**, *41*, 1399.
[3] D. Seebach, J. Gardiner, *Acc. Chem. Res.* **2008**, *41*, 1366.
[4] T. A. Martinek, F. Fulop, *Chem. Soc. Rev.* **2012**, *41*, 687.
[5] S. J. Shandler, I. V. Korendovych, D. T. Moore, K. B. Smith-Dupont, C. N. Streu, R. I. Litvinov, P. C. Billings, F. Gai, J. S. Bennett, W. F. DeGrado, *J. Am. Chem. Soc.* **2011**, *133*, 12378.
[6] K. Gademann, M. Ernst, D. Hoyer, D. Seebach, *Angew. Chem.* **1999**, *111*, 1302; *Angew. Chem. Int. Ed.* **1999**, *38*, 1223.
[7] J. A. Kritzer, M. E. Hodsdon, A. Schepartz, *J. Am. Chem. Soc.* **2005**, *127*, 4118.
[8] J. A. Kritzer, J. D. Lear, M. E. Hodsdon, A. Schepartz, *J. Am. Chem. Soc.* **2004**, *126*, 9468.
[9] J. A. Kritzer, N. W. Luedtke, E. A. Harker, A. Schepartz, *J. Am. Chem. Soc.* **2005**, *127*, 14584.
[10] J. Michel, E. A. Harker, J. Tirado-Rives, W. L. Jorgensen, A. Schepartz, *J. Am. Chem. Soc.* **2009**, *131*, 6356.
[11] A. D. Bautista, J. S. Appelbaum, C. J. Craig, J. Michel, A. Schepartz, *J. Am. Chem. Soc.* **2010**, *132*, 2904.
[12] E. F. Lee, J. D. Sadowsky, B. J. Smith, P. E. Czabotar, K. J. Peterson-Kaufman, P. M. Colman, S. H. Gellman, W. D. Fairlie, *Angew. Chem.* **2009**, *121*, 4382; *Angew. Chem. Int. Ed.* **2009**, *48*, 4318.
[13] J. D. Sadowsky, W. D. Fairlie, E. B. Hadley, H. S. Lee, N. Umezawa, Z. Nikolovska-Coleska, S. M. Wang, D. C. S. Huang, Y. Tomita, S. H. Gellman, *J. Am. Chem. Soc.* **2007**, *129*, 139.
[14] J. D. Sadowsky, M. A. Schmitt, H. S. Lee, N. Umezawa, S. M. Wang, Y. Tomita, S. H. Gellman, *J. Am. Chem. Soc.* **2005**, *127*, 11966.
[15] A. D. Bautista, O. M. Stephens, L. G. Wang, R. A. Domaoal, K. S. Anderson, A. Schepartz, *Bioorg. Med. Chem. Lett.* **2009**, *19*, 3736.
[16] O. M. Stephens, S. Kim, B. D. Welch, M. E. Hodsdon, M. S. Kay, A. Schepartz, *J. Am. Chem. Soc.* **2005**, *127*, 13126.
[17] L. M. Johnson, W. S. Horne, S. H. Gellman, *J. Am. Chem. Soc.* **2011**, *133*, 10038.
[18] Y. Imamura, N. Watanabe, N. Umezawa, T. Iwatsubo, N. Kato, T. Tomita, T. Higuchi, *J. Am. Chem. Soc.* **2009**, *131*, 7353.
[19] L. Fulop, I. M. Mandity, G. Juhasz, V. Szegedi, A. Hetenyi, E. Weber, Z. Bozso, D. Simon, M. Benko, Z. Kiraly, T. A. Martinek, *PloS One* **2012**, *7*, e39485.
[20] R. P. Cheng, W. F. DeGrado, *J. Am. Chem. Soc.* **2002**, *124*, 11564.
[21] J. L. Goodman, E. J. Petersson, D. S. Daniels, J. X. Qiu, A. Schepartz, *J. Am. Chem. Soc.* **2007**, *129*, 14746.
[22] W. S. Horne, J. L. Price, J. L. Keck, S. H. Gellman, *J. Am. Chem. Soc.* **2007**, *129*, 4178.
[23] M. W. Giuliano, W. S. Horne, S. H. Gellman, *J. Am. Chem. Soc.* **2009**, *131*, 9860.
[24] J. L. Price, W. S. Horne, S. H. Gellman, *J. Am. Chem. Soc.* **2007**, *129*, 6376.
[25] T. A. Martinek, A. Hetenyi, L. Fulop, I. M. Mandity, G. K. Toth, I. Dekany, F. Fulop, *Angew. Chem.* **2006**, *118*, 2456; *Angew. Chem. Int. Ed.* **2006**, *45*, 2396.
[26] F. Rua, S. Boussert, T. Parella, I. Diez-Perez, V. Branchadell, E. Giralt, R. M. Ortuno, *Org. Lett.* **2007**, *9*, 3643.
[27] E. Torres, E. Gorrea, K. K. Burusco, E. Da Silva, P. Nolis, F. Rua, S. Boussert, I. Diez-Perez, S. Dannenberg, S. Izquierdo, E. Giralt, C. Jaime, V. Branchadell, R. M. Ortuno, *Org. Biomol. Chem.* **2010**, *8*, 564.
[28] T. A. Martinek, I. M. Mandity, L. Fulop, G. K. Toth, E. Vass, M. Hollosi, E. Forro, F. Fulop, *J. Am. Chem. Soc.* **2006**, *128*, 13539.
[29] G. Angelici, G. Falini, H. J. Hofmann, D. Huster, M. Monari, C. Tomasini, *Chem. Eur. J.* **2009**, *15*, 8037.
[30] I. M. Mandity, E. Weber, T. A. Martinek, G. Olajos, G. K. Toth, E. Vass, F. Fulop, *Angew. Chem.* **2009**, *121*, 2205; *Angew. Chem. Int. Ed.* **2009**, *48*, 2171.
[31] L. Berlicki, L. Pilsl, E. Weber, I. M. Mandity, C. Cabrele, T. A. Martinek, F. Fulop, O. Reiser, *Angew. Chem.* **2012**, *124*, 2251; *Angew. Chem. Int. Ed.* **2012**, *51*, 2208.
[32] L. E. Townsley, W. A. Tucker, S. Sham, J. F. Hinton, *Biochemistry* **2001**, *40*, 11676.
[33] E. Szolnoki, A. Hetenyi, T. A. Martinek, Z. Szakonyi, F. Fulop, *Org. Biomol. Chem.* **2012**, *10*, 255.
[34] P. I. Arvidsson, N. S. Ryder, H. M. Weiss, G. Gross, O. Kretz, R. Woessner, D. Seebach, *ChemBioChem* **2003**, *4*, 1345.
[35] A. Chakrabartty, A. J. Doig, R. L. Baldwin, *Proc. Natl. Acad. Sci. USA* **1993**, *90*, 11332.
[36] S. A. Hart, A. B. F. Bahadoor, E. E. Matthews, X. Y. J. Qiu, A. Schepartz, *J. Am. Chem. Soc.* **2003**, *125*, 4022.
[37] R. A. Brown, T. Marcelli, M. De Poli, J. Sola, J. Clayden, *Angew. Chem.* **2012**, *124*, 1424; *Angew. Chem. Int. Ed.* **2012**, *51*, 1395.
[38] Y. Demizu, M. Doi, Y. Sato, M. Tanaka, H. Okuda, M. Kurihara, *Chem. Eur. J.* **2011**, *17*, 11107.
[39] Bruker Topspin software package for NMR data analysis.
[40] M. J. Frisch, G. W. Trucks, H. B. Schlegel, G. E. Scuseria, M. A. Robb, J. R. Cheeseman, G. Scalmani, V. Barone, B. Mennucci, G. A. Petersson, H. Nakatsuji, M. Caricato, X. Li, H. P. Hratchian, A. F. Izmaylov, J. Bloino, G. Zheng, J. L. Sonnenberg, M. Hada, M. Ehara, K. Toyota, R. Fukuda, J. Hasegawa, M. Ishida, T. Nakajima, Y. Honda, O. Kitao, H. Nakai, T. Vreven, J. A. Montgomery, Jr., J. E. Peralta, F. Ogliaro, M. Bearpark, J. J. Heyd, E. Brothers, K. N. Kudin, V. N. Staroverov, R. Kobayashi, J. Normand, K. Raghavachari, A. Rendell, J. C. Burant, S. S. Iyengar, J. Tomasi, M. Cossi, N. Rega, J. M. Millam, M. Klene, J. E. Knox, J. B. Cross, V. Bakken, C. Adamo, J. Jaramillo, R. Gomperts, R. E. Stratmann, O. Yazyev, A. J. Austin, R. Cammi, C. Pomelli, J. W. Ochterski, R. L. Martin, K. Morokuma, V. G. Zakrzewski, G. A. Voth, P. Salvador, J. J. Dannenberg, S. Dapprich, A. D. Daniels, Ö. Farkas, J. B. Foresman, J. V. Ortiz, J. Cioslowski, D. J. Fox, *Gaussian 09*, revision A.01, Gaussian, Inc., Wallingford, CT, **2009**.

Received: December 4, 2012
Published Online: April 3, 2013

